ELSEVIER

Engineering Analysis with Boundary Elements 23 (1999) 777–786

ENGINEERING ANALYSIS *with* BOUNDARY ELEMENTS

www.elsevier.com/locate/enganabound

Research note

Green's functions for the Laplace equation in a 3-layer medium, boundary element integrals and their application to cathodic protection

V.S. Ramanan[1], M. Muthukumar[2], S. Gnanasekaran, M.J. Venkataramana Reddy, B. Emmanuel*

Modelling and Simulation Group, Central Electrochemical Research Institute, Karaikudi, Tamil Nadu 630 006, India

Received 3 June 1998; accepted 19 July 1999

Abstract

We report in this paper a set of nine Green's functions for the Laplace equation for an infinite 3-layer medium in which a layer of finite width is sandwiched between two semi-infinite domains. Typical 3D plots of these Green's functions are computed and presented. Taking an offshore platform as a prime example of a structure in a 3-layer medium (atmosphere, ocean and soil), we work out the boundary element integrals using macro elements such as the tubulars. Constant elements reduce several of these boundary integrals to analytical forms. As an application, we discuss the cathodic protection modelling of offshore structures using the 'boundary element method'.

Keywords: Boundary element method; Green's functions; Cathodic protection; Laplace equation

1. Introduction

Green's functions are central to the Boundary Element Method (BEM) [1–5]. For the isotropic medium, the Green's functions associated with the Laplace equation are known to be $(r/2)$, $(1/2\pi)\ln(1/r)$ and $(1/4\pi r)$ for one, two and three dimensions, respectively. Green's functions for the Laplace equation and associated boundary element integrals are reported in this paper for a 3-layer medium in which a layer of finite width is sandwiched between two semi-infinite domains. This problem is characterised by the multi-layered nature and the infinite geometry of the solution space. One way of dealing with the multi-layers is that of zones wherein the problem is solved separately in each zone and the solutions are matched at the zone boundaries. However, the Green's function approach has the following benefits. The Green's functions have the matching conditions already built into them. Consequently, these Green's functions and the associated boundary element integrals need to be computed only once and can be re-used through iterations and for changed boundary conditions. In addition, the present approach does not require putting any fictitious enclosure to take care of the conditions at infinity.

The paper is organised as follows. In Section 2, we present a set of nine Green's functions for the Laplace equation in a 3-layer medium and also provide their 3D plots. Section 3 contains a panorama of boundary element integrals for a tubular structure embedded in a 3-layer medium. We discuss in Section 4 an application to cathodic protection modelling of offshore structures.

2. Green's functions

The 3-layer medium consists of a layer of width Δ sandwiched between two other semi-infinite layers. Our Green's functions satisfy the differential equation

$$\nabla(K\nabla G) = -\delta(x - x_s)\delta(y - y_s)\delta(z - z_s) \tag{1}$$

and obey the equations of continuity for G and $K\nabla G$ at phase boundaries. $K = K(y)$ is a piece-wise constant function exhibiting a simple discontinuity at the phase boundaries at $y = y_1$ and $y = y_{-1}$. Fig. 1 represents a 3-layer medium (for purposes of this paper, K will be interpreted as the electrical conductivity).

Eq. (1) is non-homogeneous because of the singularity at the source point (x_s, y_s, z_s). However, if the field point (x, y, z) is away from this singularity it reduces to the

* Corresponding author. Tel.: +91-4565-22368; fax: +91-4565-37779.
E-mail address: cecrik@cscecri.ren.nic.in (B. Emmanuel)
[1] Present address: Department of Chemical Engineering University of South Carolina.
[2] Gates Computer Science, Stanford, CA 94305, USA.

0955-7997/99/$ - see front matter
PII: S0955-7997(99)00025-9

Table 1
Green's functions for the 3-layer medium

1. y_s *is in the middle layer*:
(a)

$-\infty < y \leq y_{-1}$

$$G = \int_0^\infty [(k_0 + k_1)\exp(-h(y_s - y)) + (k_0 - k_1)\exp(-h(2y_1 - y_s - y))]\frac{J_0(hr)}{2\pi \det A}\mathrm{d}h$$

where
$\det A = (k_0 + k_1)(k_0 + k_{-1}) + (k_0 - k_{-1})(k_1 - k_0)\exp - 2h\Delta$

$\Delta = y_1 - y_{-1}$

and
$r = \sqrt{(x - x_s)^2 + (z - z_s)^2}$

(*b*)

$y_{-1} < y \leq y_1$

$$G = \frac{1}{4\pi R k_0} + \int_0^\infty [(k_0 - k_1)(k_0 - k_{-1})\exp\ - h[2\Delta + y_s - y] + (k_0 - k_1)(k_0 + k_{-1})\exp - h[2y_1 - y_s - y]]\frac{J_0(hr)}{4\pi k_0 \det A}\mathrm{d}h$$

$$+ \int_0^\infty [(k_0 - k_{-1})(k_0 + k_1)\exp - h[y_s - 2y_{-1} + y] + (k_0 - k_1)(k_0 - k_{-1})\exp - h[2\Delta + y - y_s]]\frac{J_0(hr)}{4\pi k_0 \det A}\mathrm{d}h$$

where

$R = \sqrt{r^2 + (y - y_s)^2}$

(*c*)

$y_1 < y < \infty$

$$G = \int_0^\infty [(k_0 - k_{-1})\exp - h[y_s + y - 2y_{-1}] + (k_0 + k_{-1})\exp - h[y - y_s]]\frac{J_0(hr)}{2\pi \det A}\mathrm{d}h$$

II. y_s *is in the bottom layer:*
(a)

$-\infty < y \leq y_{-1}$

$$G = \frac{1}{4\pi k_{-1} R} + \int_0^\infty [(k_0 + k_1)(k_{-1} - k_0)\exp\ - h[2y_{-1} - y_s - y] + (k_0 - k_1)(k_0 + k_{-1})\exp\ - h[2y_1 - y_s - y]]\frac{J_0(hr)}{4\pi k_{-1} \det A}\mathrm{d}h$$

(*b*)

$y_{-1} < y \leq y_1$

$$G = \int_0^\infty [(k_0 - k_1)\exp - h[2y_1 - y_s - y] + (k_0 + k_1)\exp\ - h[y - y_s]]\frac{J_0(hr)}{2\pi \det A}\mathrm{d}h$$

(*c*)

$y_1 < y < \infty$

$$G = \int_0^\infty k_0 \exp\ - h[y - y_s]\frac{J_0(hr)}{\pi \det A}\mathrm{d}h$$

Table 1 (*continued*)

III. y_s *is in the top layer*

(a)

$-\infty < y < y_{-1}$

$$G = \int_0^\infty k_0 \exp\ -h[y_s - y]\frac{J_0(hr)}{\pi \det A}\mathrm{d}h$$

(*b*)

$y_{-1} < y \leq y_1$

$$G = \frac{(k_0 - k_{-1})}{2\pi}\int_0^\infty \frac{\exp\ -h[y_s - 2y_{-1} + y]}{\det A}J_0(hr)\,\mathrm{d}h + \frac{(k_0 + k_{-1})}{2\pi}\int_0^\infty \frac{\exp\ -h[y_s - y]}{\det A}J_0(hr)\,\mathrm{d}h$$

(*c*).

$y_1 < y < \infty$

$$G = \frac{1}{4\pi k_1 R} + \int_0^\infty [(k_0 + k_{-1})(k_1 - k_0)\exp\ -h[y_s - 2y_1 + y] + (k_0 + k_1)(k_0 - k_{-1})\exp\ -h[y_s - 2y_{-1} + y]]\frac{J_0(hr)}{4\pi k_1 \det A}\mathrm{d}h.$$

homogeneous equation

$$\nabla^2 G = 0. \tag{2}$$

Hence, the method of finding G consists in finding the general solution to this homogeneous equation and a particular solution of the non-homogeneous part

$$K_s \nabla^2 G = -\delta(x - x_s)\delta(y - y_s)\delta(z - z_s) \tag{3}$$

where K_s is the conductivity of the layer where the source point (x_s, y_s, z_s) is located.

G is a function of the source point (x_s, y_s, z_s) and the field point (x, y, z). There are three major cases corresponding to the placement of the source point in one of the 3-layers, in turn. To each one of these cases there corresponds three further cases depending on the placement of the field point in one of the 3-layers, in turn. Thus, there are totally nine cases to be distinguished. In order to conserve space, the detailed derivations of the Green's functions are omitted. We merely list in Table 1 the set of nine Green's functions. Their 3D plots are presented in Figs. 2 and 3 for typical settings of the source point and selected ranges for the field point.

Fig. 2a exhibits first order discontinuities at the phase boundaries, while they disappear if the conductivities are equalised as in Fig. 2b. The singularities are also to be noted. In general a Green's function may have two parts, one singular and the other non-singular. The part which involves the Bessel function J_0 is not singular except when the source point is at one of the phase boundaries. Hence to avoid this singularity source point should be placed a little distance away from the phase boundary. However the $(1/R)$ part of the Green's function is singular at the source point irrespective of whether the source point is at the phase boundary or not. In this paper singularities are taken care of either by analytical integration or by the proper choice of the position of the source point.

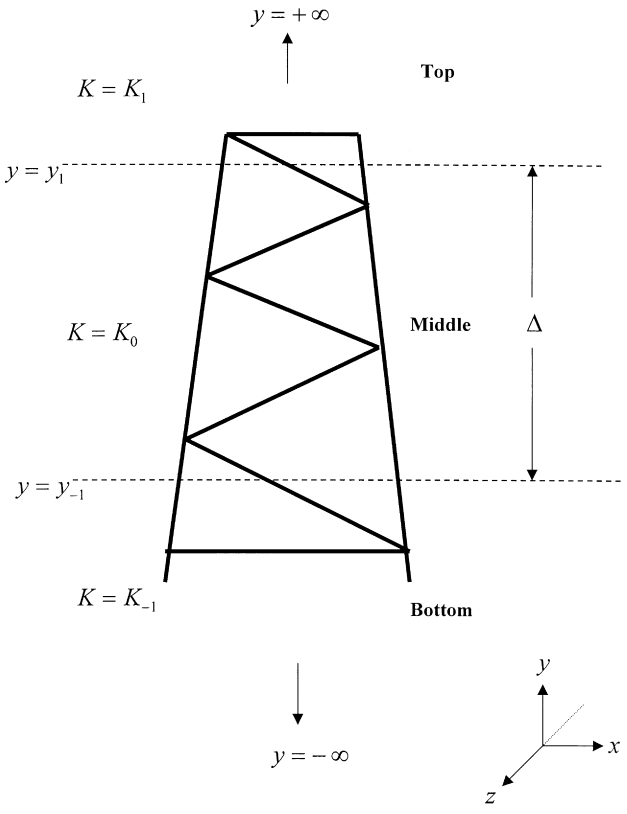

Fig. 1. A symbolic representation of a 3-layer medium of three different conductivities K_1, K_0, K_{-1}.

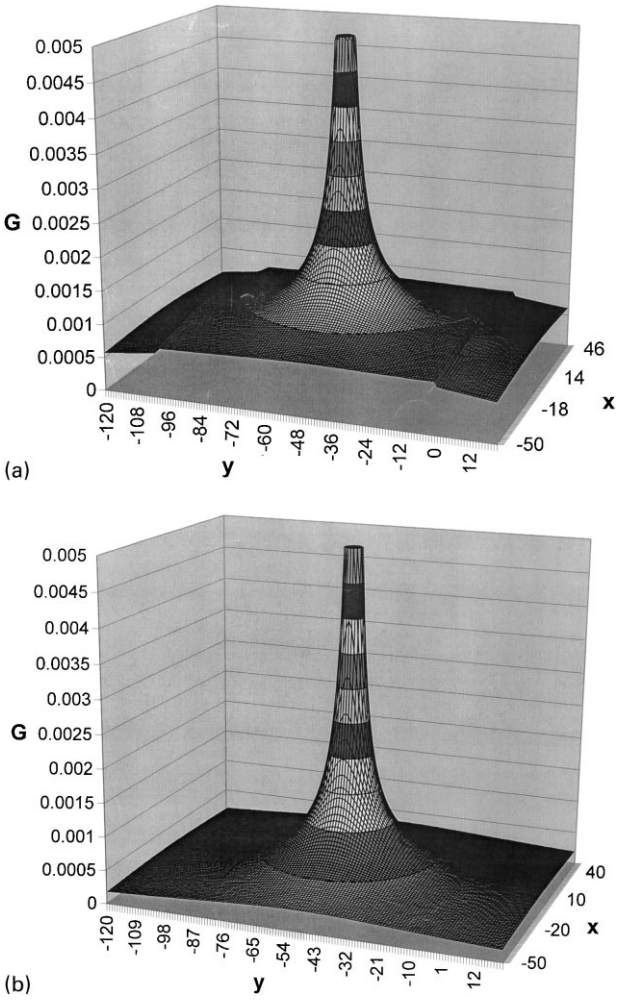

Fig. 2. (a) $y_1 = 0, y_{-1} = -100; x_s = 0, y_s = -50, z_s = 0; K_1 = 0.5, K_0 = 5, K_{-1} = 1.25$ First order discontinuities at $y = 0$ and $y = -100$ are to be noted; (b) parameters same as that of (a), except $K_1 = K_0 = K_{-1} = 5$.

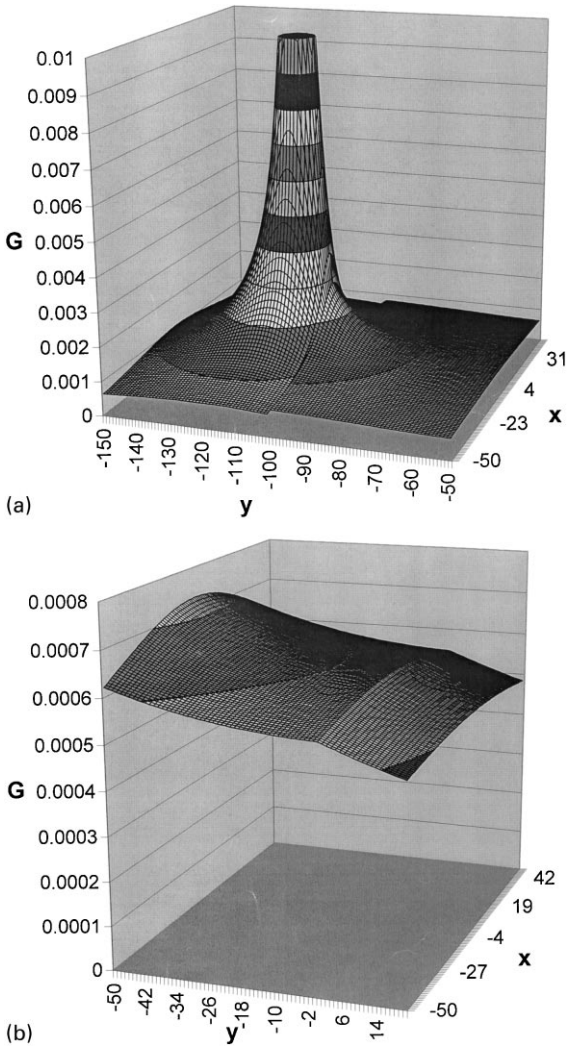

Fig. 3. (a) $y_1 = 0, y_{-1} = -100; x_s = 0, y_s = -110, z_s = 0; K_1 = 0.5, K_0 = 5, K_{-1} = 1.25$ A first order discontinuity at $y = -100$ is to be noted. (b) $y_1 = 0,\ y_{-1} = -100;\ x_s = 0,\ y_s = -110,\ z_s = 0;\ K_1 = 0.5,\ K_0 = 5,\ K_{-1} = 1.25$ A first order discontinuity at $y = 0$ is to be noted.

3. Boundary element integrals for a tubular structure in a 3-layer medium

A general tubular structure consists of a set of tubes, which may be of different diameters and a set of nodes where the tubes meet. A natural choice of boundary elements for the tubular structure would be to use tubular elements for the tubes and spherical elements (with suitably chosen effective radii) for the nodes[3]. Further, we employ only constant elements for their analytical advantage. Nonetheless, our Green's functions can be used to compute higher-order boundary element integrals also. To sum up, in this work we discretise the structure into two types of macro boundary elements: tubular and spherical elements. While each tubular element will be characterised by its terminal co-ordinates (x_0, y_0, z_0) and (x_1, y_1, z_1) and its radius, each spherical element will be characterised by its central co-ordinates (x_0, y_0, z_0) and its radius r.

If the structure is divided into N boundary elements, the discretised BEM equation is

$$C_s\phi_s^i + \sum_{j=1}^{N} H_{ij}\phi^j - \phi_\infty = \sum_{j=1}^{N} G_{ij}q^j \tag{4}$$

where

$$q^j = K\frac{\partial \phi}{\partial n} \tag{5}$$

$$G_{ij} = \int_{s_j}\int G(i,j)\,\mathrm{d}s_j \tag{6}$$

$$H_{ij} = \int_{s_j}\int K[\vec{n}\nabla G(i,j)]\,\mathrm{d}s_j \tag{7}$$

[3] Micromeshing, though it could provide a more realistic representation of the nodes, is beyond the scope of this paper.

Table 2
A panorama of BEM integrals for the source point located in the (2a) bottom, (2b) middle and the (2c) top layers

2b				G_{ij}
1	Bottom	Sphere	$i=j$	$\frac{1}{4\pi k_{-1}} f_3 + \frac{(k_0+k_1)(k_{-1}-k_0)}{4\pi k_{-1}} f_4(-P_4) + \frac{(k_0-k_1)(k_{-1}+k_0)}{4\pi k_{-1}} f_4(P_2)$
2	Bottom	Sphere	$i\neq j$	$\frac{1}{4\pi k_{-1}} f_5 + \frac{(k_0+k_1)(k_{-1}-k_0)}{4\pi k_{-1}} f_1(-P_4) + \frac{(k_0-k_1)(k_{-1}+k_0)}{4\pi k_{-1}} f_1(P_2)$
3	Bottom	Cylinder	$i=j$	$\frac{1}{4\pi k_{-1}} f_6 + \frac{(k_0+k_1)(k_{-1}-k_0)}{4\pi k_{-1}} f_2(-P_4) + \frac{(k_0-k_1)(k_{-1}+k_0)}{4\pi k_{-1}} f_2(P_2)$
4	Bottom	Cylinder	$i\neq j$	$\frac{1}{4\pi k_{-1}} f_7 + \frac{(k_0+k_1)(k_{-1}-k_0)}{4\pi k_{-1}} f_2(-P_4) + \frac{(k_0-k_1)(k_{-1}+k_0)}{4\pi k_{-1}} f_2(P_2)$
5	Middle	Sphere	$i\neq j$	$\frac{(k_0-k_1)}{2\pi} f_1(P_2) + \frac{(k_0+k_1)}{2\pi} f_1(-P_1)$
6	Middle	Cylinder	$i\neq j$	$\frac{(k_0-k_1)}{2\pi} f_2(P_2) + \frac{(k_0+k_1)}{2\pi} f_2(-P_1)$
7	Top	Sphere	$i\neq j$	$\frac{k_0}{\pi} f_1(-P_1)$
8	Top	Cylinder	$i\neq j$	$\frac{k_0}{\pi} f_2(-P_1)$
2b				
9	Bottom	Sphere	$i\neq j$	$\frac{(k_0+k_1)}{2\pi} f_1(P_1) + \frac{(k_0-k_1)}{2\pi} f_1(P_2)$
10	Bottom	Cylinder	$i\neq j$	$\frac{(k_0+k_1)}{2\pi} f_2(P_1) + \frac{(k_0-k_1)}{2\pi} f_2(P_2)$
11	Middle	Sphere	$i=j$	$\frac{(k_0-k_1)(k_0-k_{-1})}{4\pi k_0} f_4(P_3) + \frac{(k_0-k_1)(k_0+k_{-1})}{4\pi k_0} f_4(P_2) + \frac{(k_0-k_{-1})(k_0+k_1)}{4\pi k_0} f_4(P_4) + \frac{(k_0-k_1)(k_0-k_{-1})}{4\pi k_0} f_4(P_5) + \frac{1}{4\pi k_0} f_3$
12	Middle	Sphere	$i\neq j$	$\frac{(k_0-k_1)(k_0-k_{-1})}{4\pi k_0} f_1(P_3) + \frac{(k_0-k_1)(k_0+k_{-1})}{4\pi k_0} f_1(P_2) + \frac{(k_0-k_{-1})(k_0+k_1)}{4\pi k_0} f_1(P_4) + \frac{(k_0-k_1)(k_0-k_{-1})}{4\pi k_0} f_1(P_5) + \frac{1}{4\pi k_0} f_5$
13	Middle	Cylinder	$i=j$	$\frac{(k_0-k_1)(k_0-k_{-1})}{4\pi k_0} f_2(P_3) + \frac{(k_0-k_1)(k_0+k_{-1})}{4\pi k_0} f_2(P_2) + \frac{(k_0-k_{-1})(k_0+k_1)}{4\pi k_0} f_2(P_4) + \frac{(k_0-k_1)(k_0-k_{-1})}{4\pi k_0} f_2(P_5) + \frac{1}{4\pi k_0} f_6$
14	Middle	Cylinder	$i\neq j$	$\frac{(k_0-k_1)(k_0-k_{-1})}{4\pi k_0} f_2(P_3) + \frac{(k_0-k_1)(k_0+k_{-1})}{4\pi k_0} f_2(P_2) + \frac{(k_0-k_{-1})(k_0+k_1)}{4\pi k_0} f_2(P_4) + \frac{(k_0-k_1)(k_0-k_{-1})}{4\pi k_0} f_2(P_5) + \frac{1}{4\pi k_0} f_7$
15	Top	Sphere	$i\neq j$	$\frac{(k_0-k_{-1})}{2\pi} f_1(P_4) + \frac{(k_0+k_{-1})}{2\pi} f_1(-P_1)$

Table 2 (*continued*)

2b				G_{ij}
16	Top	Cylinder	$i \neq j$	$\frac{(k_0 - k_{-1})}{2\pi} f_2(P_4) + \frac{(k_0 + k_{-1})}{2\pi} f_2(-P_1)$
2c				
17	Bottom	Sphere	$i \neq j$	$\frac{k_0}{\pi} f_1(P_1)$
18	Bottom	Cylinder	$i \neq j$	$\frac{k_0}{\pi} f_2(P_1)$
19	Middle	Sphere	$i \neq j$	$\frac{(k_0 - k_{-1})}{2\pi} f_1(P_4) + \frac{(k_0 + k_{-1})}{2\pi} f_1(P_1)$
20	Middle	Cylinder	$i \neq j$	$\frac{(k_0 - k_{-1})}{2\pi} f_2(P_4) + \frac{(k_0 + k_{-1})}{2\pi} f_2(P_1)$
21	Top	Sphere	$i = j$	$\frac{1}{4\pi k_1} f_3 + \frac{(k_0 + k_{-1})(k_1 - k_0)}{4\pi k_1} f_4(-P_2) + \frac{(k_0 + k_1)(k_0 - k_{-1})}{4\pi k_1} f_4(P_4)$
22	Top	Sphere	$i \neq j$	$\frac{1}{4\pi k_1} f_5 + \frac{(k_0 + k_{-1})(k_1 - k_0)}{4\pi k_1} f_1(-P_2) + \frac{(k_0 + k_1)(k_0 - k_{-1})}{4\pi k_1} f_1(P_4)$
23	Top	Cylinder	$i = j$	$\frac{1}{4\pi k_1} f_6 + \frac{(k_0 + k_{-1})(k_1 - k_0)}{4\pi k_1} f_2(-P_2) + \frac{(k_0 + k_1)(k_0 - k_{-1})}{4\pi k_1} f_2(P_4)$
24	Top	Cylinder	$i \neq j$	$\frac{1}{4\pi k_1} f_7 + \frac{(k_0 + k_{-1})(k_1 - k_0)}{4\pi k_1} f_2(-P_2) + \frac{(k_0 + k_1)(k_0 - k_{-1})}{4\pi k_1} f_2(P_4)$

where i and j are labels of boundary elements and each vary from 1 to N.

The extra variable ϕ_∞(the potential at infinity) is to be found by extending the $N \times N$set of equations into an $(N + 1) \times (N + 1)$ set by including the total charge conservation condition whose discrete version is

$$\sum_{j=1}^{N} A_j q^j = 0 \tag{8}$$

where, $A_j$is the area of jth Boundary Element, $q^j$is current density on the jth Boundary Element. This condition ensures that no charge flux escapes to infinity.

In general the Green's function G can be split into two terms, one corresponding to the isotropic Green's function

$$G_0 = \frac{1}{R} \tag{9}$$

where

$$R = \sqrt{(x - x_s)^2 + (y - y_s)^2 + (z - z_s)^2} \tag{10}$$

and another corresponding to a sum of integrals of the following general form:

$$G_1 = \sum_{n=0}^{\infty} \frac{C_3^n}{C_1} \int_0^{\infty} \exp(-h(a' + b'y + 2n\Delta)) J_0(h\bar{r})\, \mathrm{d}h \tag{11}$$

where

$$\bar{r} = \sqrt{(x - x_s)^2 + (z - z_s)^2} \tag{12}$$

and J_0 is the Bessel function of the zeroth order.

Using an identity [6], this is further reduced to the following form:

$$G_1 = \sum_{n=0}^{\infty} \frac{C_3^n}{C_1} \frac{1}{R_n} \tag{13}$$

where

$$R_n = \sqrt{(x - x_s)^2 + (a' + b'y + 2n\Delta)^2 + (z - z_s)^2} \tag{14}$$

.

The boundary integrals H_{ij}s and G_{ij}s are now classified depending on whether $i = j$ or $i \neq j$ and whether the field point (integration point j) ranges over a tubular or a spherical element. Also, the integration over the G_0 part and the G_1 part of the Green's function must be treated separately. As there are nine types of Green's functions (cf. Section 2),

Table 3
The list of the seven function routines f_is and f_i's and the five parameters p_is

Function f_1

$$f_1 = \frac{4\pi r^2}{C_1}\sum_{n=0}^{\infty} C_3^n \frac{1}{R_n}$$

$$f_1' = \sum_{n=0}^{\infty} \frac{4\pi r^2}{LR_n^3}\frac{C_3^n}{C_1}[-(x_s - x_0)(x_s - x) + b'(y_s - y_0)(a' + b'y + 2n\Delta) - (z_s - z_0)(z_s - z)]$$

where

$$x = \frac{(x_s - x_0)r}{L} + x_0$$

$$y = \frac{(y_s - y_0)r}{L} + y_0$$

$$z = \frac{(z_s - z_0)r}{L} + z_0$$

$$L = \sqrt{(x_0 - x_s)^2 + (y_0 - y_s)^2 + (z_0 - z_s)^2}$$

and

$$R_n = \sqrt{(x - x_s)^2 + (a' + b'y + 2n\Delta)^2 + (z - z_s)^2}$$

Function f_2

$$f_2 = \frac{r}{C_1}\sum_{n=0}^{\infty} C_3^n \int_0^{2\pi} \ln\left(\frac{2\sqrt{A + BL + L^2} + 2L + B}{2\sqrt{A} + B}\right) \mathrm{d}\theta$$

$$f_2' = \frac{2r}{C_1}\sum_{n=0}^{\infty} C_3^n \int_0^{2\pi} \frac{(B\sqrt{A} - (2L + B)\sqrt{A + BL + L^2} - 2L(B + L))(\ldots)\,\mathrm{d}\theta}{(2(A + BL + L^2) + (2L + B)\sqrt{A + BL + L^2})(2A + B\sqrt{A})}$$

where

$$(\ldots) = \left(\frac{a_1(x_s - x_0)}{r} + \frac{a_2(a' + b'y_0 + 2n\Delta)}{r} + \frac{a_3(z_s - z_0)}{r} + r - \frac{(x_s - x_0)^2}{r} - \frac{(a' + b'y_0 + 2n\Delta)^2}{r} - \frac{(z_s - z_0)^2}{r}\right)$$

$$A = a_1^2 + a_2^2 + a_3^2$$

$$B = 2(a_1b_1 + a_2b_2 + a_3b_3)$$

$$a_1 = (x_s - x_0) + r(-\cos\theta + c(1 - \cos\phi)(c\cos\theta + a\sin\theta)$$

$$b_1 = -c\sin\phi$$

$$a_2 = a' + b'y_0 + 2n\Delta - b'r\sin\phi(c\cos\theta + a\sin\theta)$$

$$b_2 = b'\cos\phi$$

$$a_3 = z_s - z_0 + r(\sin\theta - a(1 - \cos\phi)(c\cos\theta + a\sin\theta))$$

$$b_3 = a\sin\phi$$

$$a = \frac{-(z_1 - z_0)}{\sqrt{(z_1 - z_0)^2 + (x_1 - x_0)^2}};\quad c = \frac{x_1 - x_0}{\sqrt{(z_1 - z_0)^2 + (x_1 - x_0)^2}}$$

Table 3 (*continued*)

$\cos\phi = \dfrac{y_1 - y_0}{L}$ and $L = \sqrt{(x_1 - x_0)^2 + (y_1 - y_0)^2 + (z_1 - z_0)^2}$

Function f_3

$f_3 = 4\pi r$

$f'_3 = -4\pi$

Function f_4

$$f_4 = \frac{8\pi r^2}{C_1} \sum_{n=0}^{\infty} \frac{C_3^n}{(\sqrt{A + B} + \sqrt{A - B})}$$

$f'_4 = 0$

where

$A = r^2 + (a' + b'y_0 + 2n\Delta)^2$

$B = 2rb'(a' + b'y_0 + 2n\Delta)$

Function f_5

$f_5 = 4\pi r^2/l$

$f'_5 = 0$

where

$l = \sqrt{(x_0 - x_s)^2 + (y_0 - y_s)^2 + (z_0 - z_s)^2}$

Function f_6

$$f_6 = 2\pi r \ln\left(\frac{L - l + \sqrt{(L - l)^2 + r^2}}{-l + \sqrt{l^2 + r^2}}\right)$$

$$f'_6 = 2\pi r^2 \left(\frac{1}{L - l + \sqrt{(L - l)^2 + r^2}} \frac{1}{\sqrt{(L - l)^2 + r^2}} - \frac{1}{-l + \sqrt{l^2 + r^2}} \frac{1}{\sqrt{l^2 + r^2}}\right)$$

where

$l = \sqrt{(x_0 - x_s)^2 + (y_0 - y_s)^2 + (z_0 - z_s)^2}$

$L = \sqrt{(x_1 - x_0)^2 + (y_1 - y_0)^2 + (z_1 - z_0)^2}$

Function f_7

$$f_7 = r \int_0^{2\pi} \ln\left(\frac{2\sqrt{A + BL + L^2} + 2L + B}{2\sqrt{A} + B}\right) \mathrm{d}\theta$$

$$f'_7 = 2r \int_0^{2\pi} \frac{(B\sqrt{A} - (2L + B)\sqrt{A + BL + L^2} - 2L(B + L)(\ldots)}{(2(A + BL + L^2) + (2L + B)\sqrt{A + BL + L^2})(2A + B\sqrt{A})} \mathrm{d}\theta$$

where

$$(\ldots) = \left(\frac{a_1(x_s - x_0)}{r} + \frac{a_2(y_s - y_0)}{r} + \frac{a_3(z_s - z_0)}{r} + r - \frac{(x_s - x_0)^2}{r} - \frac{(y_s - y_0)^2}{r} - \frac{(z_s - z_0)^2}{r}\right)$$

$A = a_1^2 + a_2^2 + a_3^2$

$B = 2(a_1b_1 + a_2b_2 + a_3b_3)$

Table 3 (*continued*)

$a_1 = (x_s - x_0) + r(-\cos\theta + c(1 - \cos\phi)(c\cos\theta + a\sin\theta))$

$b_1 = -c\sin\phi$

$a_2 = (y_s - y_0) + r\sin\phi(c\cos\theta + a\sin\theta)$

$b_2 = -\cos\phi$

$a_3 = z_s - z_0 + r(\sin\theta - a(1 - \cos\phi)(c\cos\theta + a\sin\theta))$

$b_3 = a\sin\phi$

$$a = \frac{-(z_1 - z_0)}{\sqrt{(z_1 - z_0)^2 + (x_1 - x_0)^2}}; \qquad c = \frac{x_1 - x_0}{\sqrt{(z_1 - z_0)^2 + (x_1 - x_0)^2}}$$

$$\cos\phi = \frac{y_1 - y_0}{L} \text{ and } L = \sqrt{(x_1 - x_0)^2 + (y_1 - y_0)^2 + (z_1 - z_0)^2}$$

Parameters

P_i	a'	b'
P_1	y_s	-1,
P_2	$2y_1 - y_s$	-1
P_3	$2\Delta + y_s$	-1
P_4	$y_s - 2y_{-1}$	$+1$
P_5	$2\Delta - y_s$	$+1$

there is a further classification according to the placement of the source point (i index) and the field point (j index) among the three layers denoted top, middle and bottom (Fig. 1). A complete enumeration of all relevant combinations leads eventually to 24 cases for the G_{ij}s and a corresponding 24 cases for the H_{ij}s. The mathematics required for a convenient evaluation of this plethora of boundary integrals is quite tedious and involve transformations to local frames of references and symmetry arguments, the details of which we omit for the sake of brevity. A full panorama of the G_{ij}s is provided in Tables 2. In each table, the first column represents the location of the field point, the second column indicates the boundary element type over which the integration is performed and the third column tells if $i = j$ or $i \neq j$. Entries in the tables involve seven functions/routines f_i ($i =$ 1–7) (There are eight cases in principle, but two are alike.) Some of these functions have an argument P (the argument P is actually a pair of parameters a', b') which assumes one of the five values P_is ($i = 1$–5). These seven functions and the five argument values are listed separately in Table 3. This completes the panorama of G_{ij}s. From this, a corresponding panorama of H_{ij}s can be easily constructed as follows. Take each G_{ij}, replace every f_i by f_i' and multiply throughout by the conductivity of the layer in which the boundary element j is located. The derivative functions f_i's are also listed along with the f_is in Table 3.

4. Application to cathodic protection modelling of offshore structures

Cathodic protection is a well-known method of protecting metallic structures against corrosion. A fairly extensive literature is available on the application of the BEM to cathodic protection problems [7–11]. Offshore structures play an important role for the oil and gas industry. These are huge metallic structures made of tubular members and installed in deep oceans with parts exposed to the atmosphere at the top and parts running into the ocean mud at the bottom. Being in a marine environment, these structures are prone to corrosion. The 3-layer medium consisting of atmosphere, ocean and soil and an offshore structure placed in these environments provide a typical example of

problems where the results of the present paper are applicable.

The basic problem in cathodic protection is to solve the Laplace equation

$$\nabla^2\phi = 0 \tag{15}$$

for the potential distribution ϕ and the current density distribution $i = K\nabla\phi$.

Using the boundary element mathematics developed in this paper, we have successfully developed a comprehensive software package for cathodic protection modelling of offshore structures, in a collaborative project with the Oil and Natural Gas Corporation of India. This software, named CPSEA + +, was developed using GNU's C + + and Turbo C + +. The processor runs on native Linux environment while the pre-processor, the post-processor and the other tools are based on the Disk Operating System. The software has been tested on several model structures, including a real offshore structure. For a typical structure discretised into 1000 boundary elements (nodes + tubes + anodes), the processor took about 3 h (on a Pentium 75 MHz system with 16 MB of RAM) for the computation of the H and G matrices and nearly half-an-hour for the multi-dimensional Newton–Raphson iterative solution of the BEM equation incorporating a non-linear boundary condition for the structure and a Dirichlet's for the sacrificial anodes.

Acknowledgements

This paper is the outcome of an in-house R&D program at the Modelling and Simulation Group of CECRI, Karaikudi, India. Permission to publish this work is gratefully acknowledged.

References

[1] Brebbia CA, Telles JCF, Wrobel LC. Boundary element techniques, theory and applications in engineering, Berlin and Heidelberg: Springer, 1984.
[2] Brebbia CA, Walker S. Boundary element techniques in engineering, London: Newnes Butterworths, 1980.
[3] Telles JCF, Wrobel LC, Mansur WJ, Azevedo JPS. In: Brebbia CA, Maier G, editors. Boundary elements VII, Berlin: Springer, 1985.
[4] Brebbia CA, Maier G, editors. Proceedings of the 7th International Conference on BEM, 1/2. Berlin: CML Publications/Springer, 1985.
[5] Ramachandran PA. Boundary element methods in transport phenomena, London: Elsevier, 1994.
[6] Gradshtegn IS, Ryzhik IM. Table of integrals, series and products, New York: Academic Press INC/Harcourt Brace Jovanovich Publishers, 1979.
[7] Danson DJ, Warne MA. Current density/voltage calculations using Boundary element techniques, NACE Conference, Los Angeles, USA, 1983.
[8] Adey RA, Niku SM, Brebbia CA, Finnegan J. Computer aided design of cathodic protection systems. Paper presented at the International Conference on Boundary Element Methods in Engineering, Villa Olmo, Lake Como, Italy, 24–27 September, 1985.
[9] Adey RA, Niku SM. Computer modelling of corrosion using the boundary element method. Computer Modelling in Corrosion. American Society of Testing and Materials Philadelphia, 1992, ASTM STP 1154. p. 248–69.
[10] Nisancioglu K. Design techniques in cathodic protection engineering. In: Conway BE, Bockris JO'M, White RE, editors. Modern aspects of electrochemistry no. 23, New York: Plenum Press, 1992. p. 149–237.
[11] Zamani NG, Porter JF, Mufti AA. A survey of computational efforts in the field of corrosion engineering. International Journal for Numerical Methods in Engineering 1986;23(7):1295–311.